

IAC-14-C4.3.2

## STATUS AND FUTURE PERSPECTIVES OF THE CMC ROCKET THRUST CHAMBER DEVELOPMENT AT DLR

**M. Ortelt**

DLR Stuttgart, Germany, [markus.ortelt@dlr.de](mailto:markus.ortelt@dlr.de)

**H. Hald, I. Mueller**

DLR Stuttgart, Germany, [Hermann.hald@dlr.de](mailto:Hermann.hald@dlr.de), [ilja.mueller@dlr.de](mailto:ilja.mueller@dlr.de)

DLR offers within its *Black Engine* program a large portfolio of fiber reinforced structure systems for functional components in rocket thrust chambers. New material classes show high application potential for several space propulsion systems, e.g. orbital space propulsion or high performance rocket engines. Load carrying structures made of CFRP (Carbon Fiber Reinforced Plastics) are of high interest focusing on high performance engines. They are promising future design candidates because of their general weight reduction potential accompanied by high material strength. CFRP load shell structures, used in representative tests, could be proved as cryogenic hydrogen tight with regard to typical test bench requirements. CMC (Ceramic Matrix Composites) materials stand in the major focal point. Firstly they are highly applicable as hot structures for inner liners in the subsonic combustion chamber component. Secondly they can be used for self-sustaining structures of supersonic nozzle extensions. Beside this typical target courses they also can be used in the injector component. Within relatively easy manufacturing processes highly sophisticated channel patterns can be applied in CMC injector elements. Apart from this constructive property CMC designs are very interesting with regard to requirements due to fabrication tolerances. Naturally CMC injector elements are suited for hot injection as well as for cold injection. A lot of CMC material development effort in the last years led to specific material selections in terms of thermo-chemical resistance under the ambitious hot gas conditions in high performance LOX/LH<sub>2</sub> operation. Beside multiple numerical works concerning cooling methods extensive test campaigns have been conducted at DLR's P8 and P6.1 test facilities. Principal goals could be reached: High efficient hot gas operation of transpiration cooled inner CMC liners in subscale LOX/LH<sub>2</sub> demonstrators (up to 90 bars chamber pressure) compared under scaling aspects [2] to standard high performance thrust chambers (Vulcain engine); Damage free operation under relevant high performance hot gas conditions (50 mm chamber, 7 % overall coolant mass flow ratio); Structurally reliable light weight design showing high ratio of thermal and mechanical load de-coupling. In matters of cooling principles all standard methods seem to be interesting in conjunction with the CMC technology. Apart from the excellently working transpiration cooling, first evaluations are ongoing considering regenerative cooled CMC wall structures, but also radiative and film cooled systems targeting on the 500 N apogee motor classes, combined with new structural design approaches, show promising perspectives for future applications.

### I. INTRODUCTION

After more than 15 years intensive investigations on transpiration cooled CMC high performance rocket thrust chamber technology it can be stated, that transpiration cooled inner CMC liners can be operated damage free and under high pressure conditions in cryogenic stage propulsion.

The porous materials themselves show homogeneously distributed open pore morphology as well as adjustable permeability for optimized coolant diffusion. The latter can be reached by discretely adjusted porosities. Additionally specific selections of inherent material composition show on the one hand adequate thermochemical resistance at the hot gas surface and on the other hand good coolant flow properties through the wall. As a consequence such inner liner components can be operated functionally

efficient without critical material degenerations even being exposed to local thermochemical load peaks.

In parallel DLR focused on CMC injector technology. Typical properties of the materials themselves or specific manufacturing properties promise functional improvements like versatile spray forming and design simplification by utilisation of specific morphology and thermo-mechanical properties focusing hybrid designs.

Appropriate manufacturing processes and structure geometries in conjunction with suitable material compositions as well as new joining technology approaches for supersonic nozzle extensions are very promising considering continuously fibre reinforced rocket thrust chamber components, which represent conclusive functional structure systems.

## II. STATUS OF INNER LINER DEVELOPMENT

Several CMC material derivatives have been investigated for transpiration cooled inner liners of LOX/LH2 (LOX/GH2-120K) operated rocket thrust chambers. Interesting candidates are given in figure 1, which fulfil principally the functional and structural requirements.

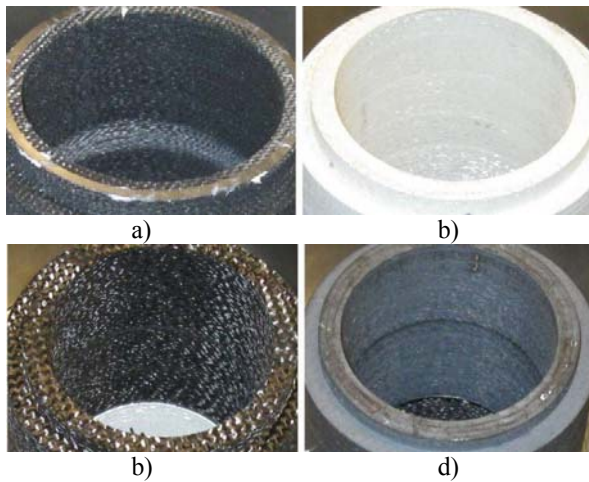


Fig. 1: CMC derivatives. a) OXIPOL (DLR); b) AvA-Z-ISC (WPS); c) C/SiCN (DLR); d) C/C (DLR), CVI coated MT-Aerospace.

The morphology of the materials themselves is an important characteristic with regard to homogeneous porosities and permeabilities. Figure 2 and 3 show SEM graphs of two important material candidates. C/C represents the material with the currently most scientific experience concerning active cooling methodology.

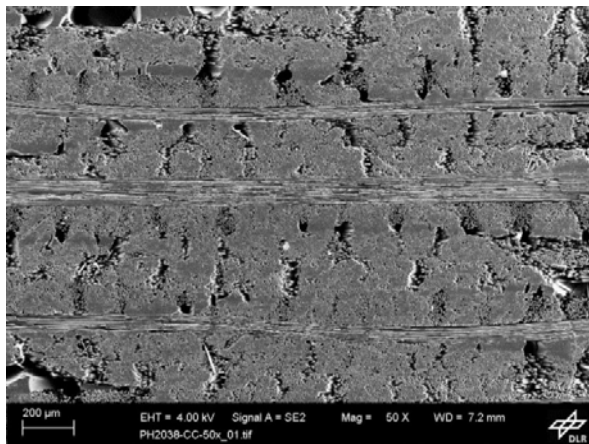


Fig. 2: SEM graph of typical DLR C/C material, showing homogeneous pore distribution

C/SiCN seems to be the most promising candidate for the transpiration cooled thrust chamber application, showing the best resistance against thermo-chemical hot gas attacks.

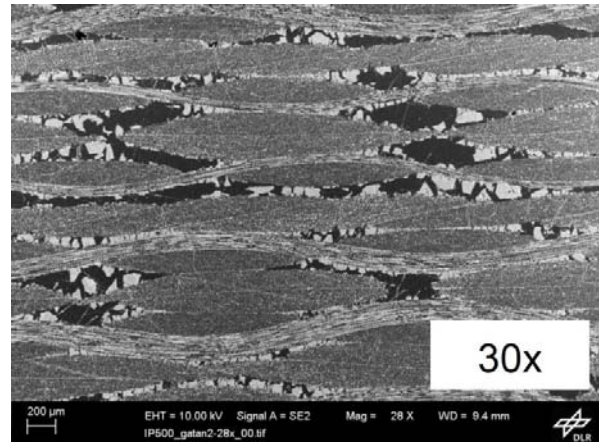


Fig. 3: SEM graph of typical DLR's C/SiCN material, showing homogeneous pore distribution and SiCN fractures inside the pores

Concerning oxide CMC derivatives one important material is given by AvA-Z-ISC [18,19], which shows high open porosity of about 34 % (fig. 4). In addition it shows good homogeneity comparable to C/C material. Hence this CMC is appropriate for the transpiration cooled thrust chamber application, in particular adjacent to the injector, where a high amount of un-burnt oxygen is expected. Within a test campaign at the European Research and Technology Test Facility P8 at DLR Lampoldshausen this material could demonstrate excellently its oxidation resistance under high performance conditions ( $p_c = 60$  bar) in a 50 mm demonstrator, in tests up to 120 s.



Fig. 4: SEM graph of oxide AvA-Z-ISC material.

Oxipol is a DLR in-house oxide material [18]. It shows oxidation resistance and porosity of about 10 %. Additionally this CMC derivative shows good permeability and homogeneity (fig. 5). It could prove its applicability in partially cryogenic tests (LOX & GH2 at 120 K) at the renewed P6.1 technology test facility at DLR Lampoldshausen.

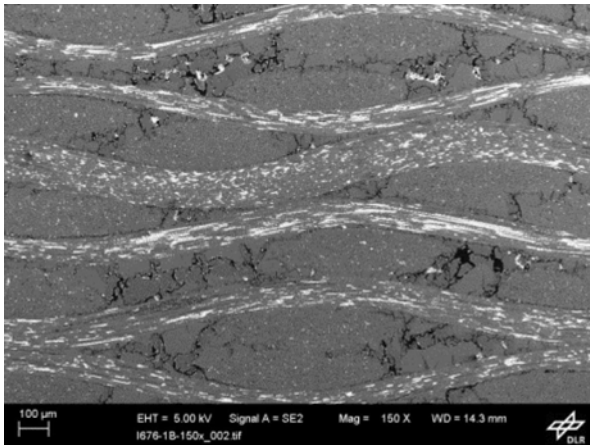


Fig. 5: SEM graph of Oxipol CMC, a DLR in-house oxide derivative.

Flow physics of porous media are currently of high interest all over the world, in particular the utilisation of porous CMC [6, 11, 12, 21]. Nowadays multiple researches are ongoing and a variety of publications can be found in this field. The transpiration principally can be described by the general Darcy-Forchheimer equation (equ. 1 and fig. 4), whereas the Forchheimer ratio considers the impact of turbulences.

$$\frac{dp}{dx} = -\left(\frac{\eta}{k_D} \cdot u + \frac{\rho}{k_F} \cdot u^2\right) \quad [1]$$

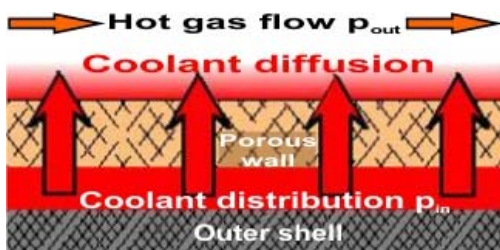


Fig. 6: Principle of the transpiration cooled porous CMC wall

The relevant characteristics of the material candidates like permeability, thermo-physical or thermo-chemical behaviour can be adjusted during the material selection or the manufacturing process. Typically the materials themselves will be produced in form of flat plates, which guaranties a high level of material quality and reproducibility. Later ring segments will be extracted.

DLRs design approach (fig. 7) allows the combination of miscellaneous materials in one inner liner component. The materials are applied in form of ring segments as mentioned which will be stacked in a row into the load carrying outer chamber housing. Hence specific materials can be chosen for adjusted placements correlating to the locally changing hot gas conditions (fig. 8) [1,3].

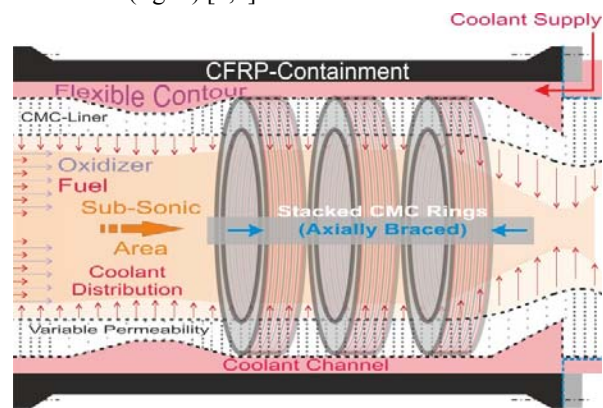


Fig. 7: DLR's specific design approach for a transpiration cooled CMC thrust chamber.

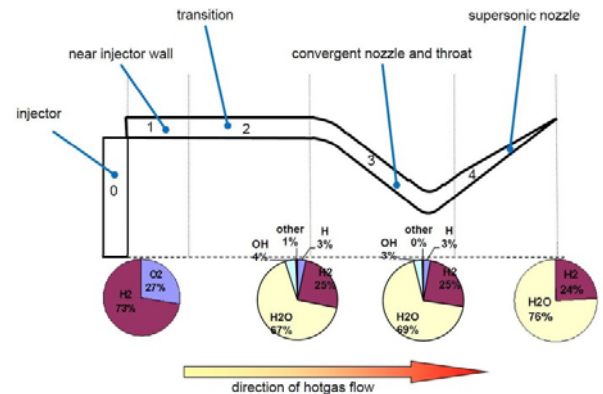


Fig. 8: Axially changing hot gas conditions in a cryogenically operated rocket thrust chamber [2].

### III. CMC MATERIAL DEVELOPMENT

The materials chosen for the thrust chamber application require specific functional features. Firstly they must have definable porosity and permeability respectively. Secondly the relevant calorimetric parameters like thermal conductivity and (thermo-)

mechanical parameters like strength, stiffness and thermal elongation must be known.

Porosity and permeability

Depending on the manufacturing process discrete porosities can be created. Considering optimized hydrogen diffusion due to experience in cryogenic thrust chamber tests porosities in the range from 6 % to 10 % seem currently to be the best fit. Consequently the specifically depending permeability can be selected for an adjusted diffusion in the porous thrust chamber liner.

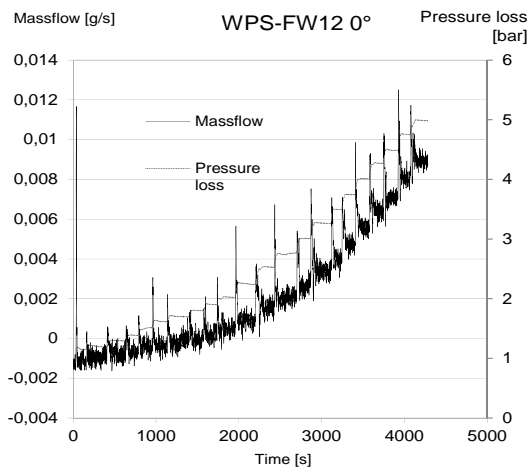


Fig. 9: Mass flow measurement depending on pressure loss levels.

Figure 9 shows a typical measurement procedure to obtain basic raw data. The mass flow, pressure drop and temperature correlation can be transformed into the  $k_d$  and  $k_f$  calculations, which will be implemented into combined flow simulations. To combine means in this case the combination of liner diffusion and hot gas flow.

For standardisation purposes a specific flow facility has been designed in conjunction with a viable specimen sizing to conduct characterization flow tests.

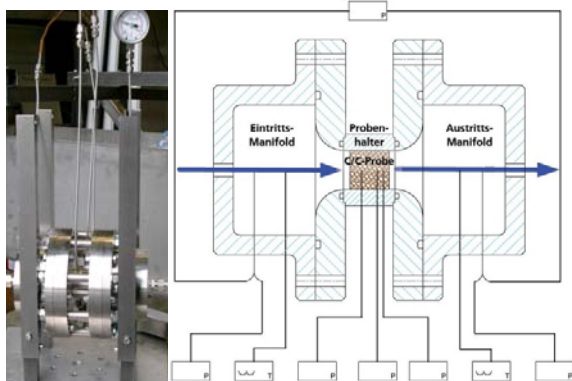


Fig. 10: Mass flow measurement device (left). Cross section view (right) [11].

The inlet and the outlet pressure as well as three inherent specimen pressures will be measured. Additionally the inlet and outlet temperature will be recorded. The orthotropy shows differences in the diffusion quantity (fig. 10, 11; 12).

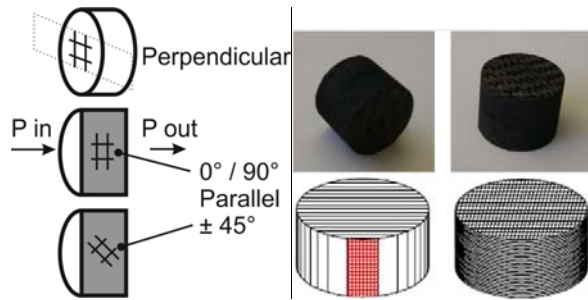


Fig. 11: Graphic illustration of the inherent orthotropic flow directions. Specimen size: 30 mm in diameter and 30 mm in height.

On the one hand significant differences can be found in the comparison of parallel and perpendicular flow (fig. 12), on the other hand the morphological difference between 0/90° and +45° flow related to the different in-plane fibre orientations show slight variance.

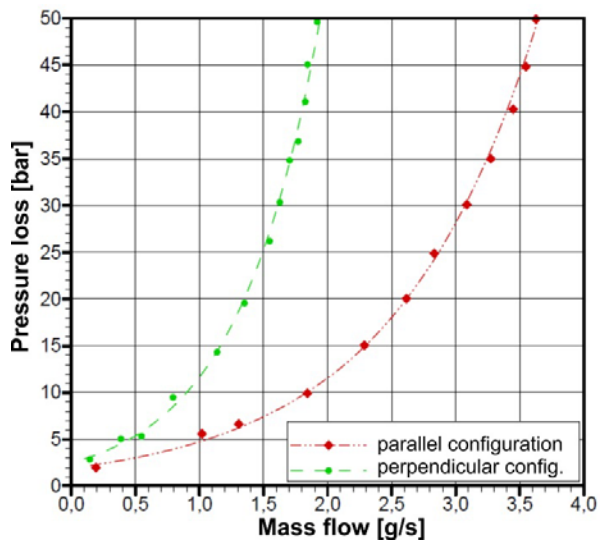


Fig. 12: Flow differences in orthotropic porous CMC at room temperature (standard C/C, 13 % open porosity), perpendicular and parallel 0/90°.

The quantitative permeability depends on the Darcy and the Forchheimer coefficients which often can be determined analytically by equations 2 and 3 [22] under simplified conditions, approximately derived by the flow through a ball fillings model morphology.

$$k_D = \frac{\varepsilon^3 \cdot d_p^2}{150 \cdot (1 - \varepsilon)^2} \quad [2]$$

$$k_F = \frac{1,75 m}{\sqrt{150 \cdot \varepsilon^3}} \quad [3]$$

But the diffusion through CMCs differs significantly from the ball filling morphology. For adequate determination of the CMC permeabilities the empirical way is constructive. For that method physical parameters (temperature, pressure, mass flow) of the diffusion have to be measured. The dynamic viscosity and density can be calculated by the general thermodynamic state equation. Subsequently the permeabilities can be determined by equation 4 [22] the better the more measurement points are gathered. The index  $r$  marks one reference condition (in-flow or out-flow).

$$\frac{p_{in}^2 - p_{out}^2}{2} = \frac{\eta}{k_D} \cdot u_r + \frac{\rho_r}{k_F} \cdot u_r^2 \quad [4]$$

Table 1 gives measured values of DLR standard C/C material which ranges at about 13 % open porosity.

|                          | $k_D \cdot e^{-13} [m^2]$ | $k_F \cdot e^{-8} [m]$ |
|--------------------------|---------------------------|------------------------|
| C/C (13 % open porosity) | 2.2424                    | 2.4355                 |

Table 1: Permeability coefficients of DLR's standard C/C material.

The values given in table 2 compare the diffusion of different media, gaseous nitrogen and gaseous hydrogen [11]. In [11] separate methodologies have been chosen.

|                           | GN2 | GH2 |
|---------------------------|-----|-----|
| $k_D \cdot e^{-13} [m^2]$ | 4.8 | 5.5 |
| $k_F \cdot e^{-8} [m]$    | 6.3 | 6.6 |

Table 2: Representative analytical values of Darcy and Forchheimer coefficients, using GN2 and GH2.

Typical anisotropy coefficients, defined by the quotient of the parallel and the perpendicular permeability, range around 3. Table 3 gives the ratios of the numerically calculated values [11].

|     | $k_{d \parallel} / k_{d \perp}$ | $k_{f \parallel} / k_{f \perp}$ |
|-----|---------------------------------|---------------------------------|
| GN2 | 3.879                           | 2.292                           |
| GH2 | 3.385                           | 2.867                           |

Table 3: Anisotropy coefficients of parallel and perpendicular flow

According to the diffusion quantification the effusion homogeneity is being investigated within an ongoing PHD thesis [6]. Concerning a homogeneous interaction of hot gas and coolant flow roughly scattered local peaks of coolant jets should be prevented. Currently multiple measurements in DLR's AORTA facility happens to optimize the materials morphology with the goal of best effusion homogeneity. Figure 13 shows the effusion pattern measured by Pitot sensor using a typical C/C specimen.

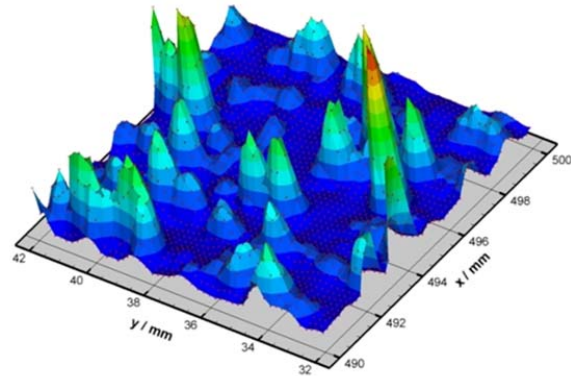


Fig. 13: Effusion homogeneity of porous C/C.

#### Classical material parameters

In conjunction with the thrust chamber designing process the following characteristics are focused: Strength, stiffness, CTE, thermal conductivity and heat capacity. It has to be considered that all properties are orthotropic, thus depending on fibre ply orientations.

The mechanical characteristics range significantly below the metallic candidates. Table 4 gives typical ranges. Additionally one important characteristic can be seen in the low CTE, which ranges between 0 and about  $6 \times 10^{-6} K$ , whereas oxide derivatives range more at the higher values.

|                                   |            |
|-----------------------------------|------------|
| Tensile strength [MPa]            | 80 - 300   |
| Compression strength [MPa]        | 200 - 1300 |
| Young's modulus [MPa]             | 50 - 230   |
| Interlaminar shear strength [MPa] | 10 - 50    |

Table 4: Ranges of mechanical properties for general CMCs

In conjunction with the CMC thrust chamber design the material compression perpendicular to the fibre plies is an important design criterion. Figure 14 shows the perpendicular compression measurement of a cubical C/C specimen (10 x 10 x 10 mm).

The measurement of the specimens shows a typical quasi-linear slope after the first compression settling. Within this slope (marked by the black rectangle) the

operational point for the pre-compression in the chamber design will be defined. The material should structurally manage the shrinkage during pre-cooling being continuously braced.

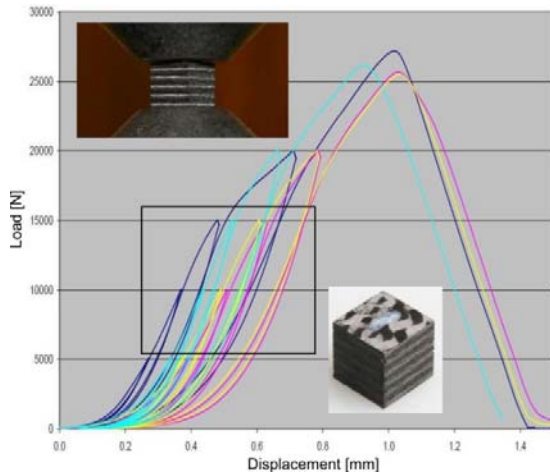


Fig. 14: Compression measurement of 4 cubical specimens (10 x 10 x 10 mm) for the definition of the operational compression point within the quasi-linear material characteristic (marked rectangle)

More important is the thermal behaviour of the CMCs. The heat capacities range generally from 90 J/KgK up to 1500 J/KgK. The thermal conductivity represents the most important thermal characteristic. Principally it can be stated that oxide CMCs show significantly lower thermal conductivities than carbon fibre or SiC fibre based derivatives.

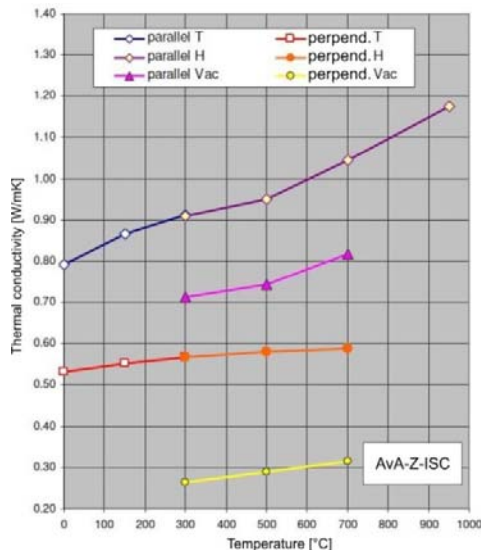


Fig. 15: Parallel and perpendicular thermal conductivities of AvA-Z-ISC material at different temperatures and atmospheres

Figure 15 gives the characteristic of AvA-Z-ISC, at typical oxide CMC, at different atmospheres, temperatures and in parallel or perpendicular orientation.

Figure 16 gives in parallel the same characteristics for the standard DLR C/C material. The thermal conductivity lies about one magnitude higher than for oxide materials.

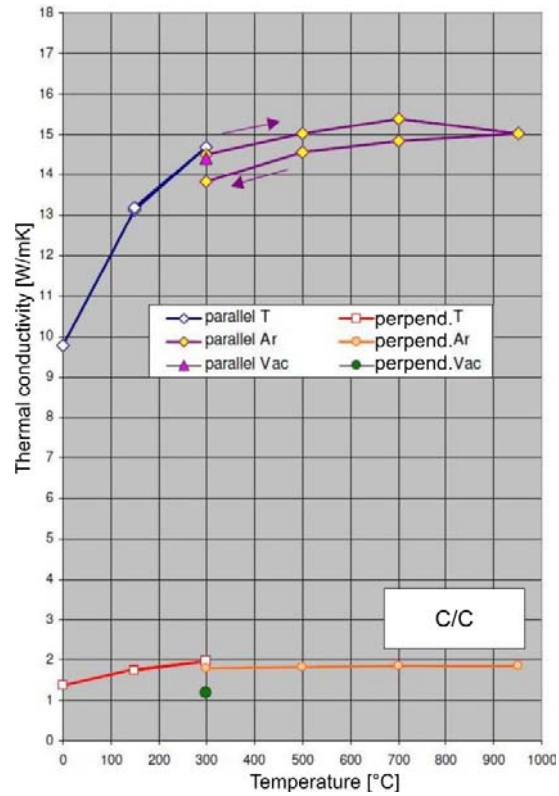


Fig. 16: Parallel and perpendicular thermal conductivities of standard DLR C/C material at different temperatures and atmospheres

Using high conductive pitch fibres the thermal conductivity can be increased significantly at ambient temperatures, but at high temperatures of more than 1000 K it can be ultimately increased up to approximately 30 W/mK, caused by temperature dependant decrease of heat capacity, which influences the thermal conductivity.

Thermo-chemical evaluation

A main disadvantage of C/C is the oxidation weakness. This material can sustain relatively high temperatures in inert gas atmosphere, but oxidizes above ~600°C. So if the atmosphere at the inner liner isn't saturated with the coolant this material is not the best choice. For that reason several new materials have been tested in the last campaigns [1, 2, 3].



Fig. 17: AvA-Z-ISC material in the oxidation critical zone close to the injector, showing tracks of hot gas attacks.

One of the materials tested was the WPS AvA-Z-ISC. It's a CMC based on aluminum oxide fibers and matrix (fig. 4, 17). This Material was placed in the mixing and combustion zone in the combustion chamber. At this location the risk of oxidation is the highest. As the material is out of aluminum oxide the main problem of C/C material was solved quite simple as the cooled structure was below the maximum temperature of 1200°C for aluminum oxide. In general there are many factors which influence the possible damages of the inner liner. The thermo- chemical and physical stresses have to be taken into account for an optimized combustion chamber. For this reason there are efforts at DLR-BT catching all the parameters and effects for a damage behavior of actively cooled CMC combustion chambers. Currently a PHD thesis is ongoing to investigate thermo-chemical effects in hot gas environment of rocket thrust chambers. Figure 6 displays a variety of typical materials investigated in the development program. As most promising candidate downstream and for inner Laval nozzle structures crystallized the C/SiCN derivative in the latest demonstration test campaigns.

#### IV. CMC INJECTOR TECHNOLOGY

The CMC injector technology is represented by a new structure approach. Figure 18 shows the structure principle of DLR's cone injector design [9].



Fig. 18: Design principle of the CMC cone injector

It consists of an alternating concentric ring-gap system, where alternately the gaps are open for the fuel (H<sub>2</sub>) injection and filled with highly propellant permeable CMC elements. In the technological first generation the conical CMC injector elements had been manufactured using hybrid woven fabrics consisting of partially oxide fibres and carbon fibres. During high temperature material consolidation in oxidizing atmosphere the carbon fibres were going lost. Figure 19 gives an overview of this design phase.

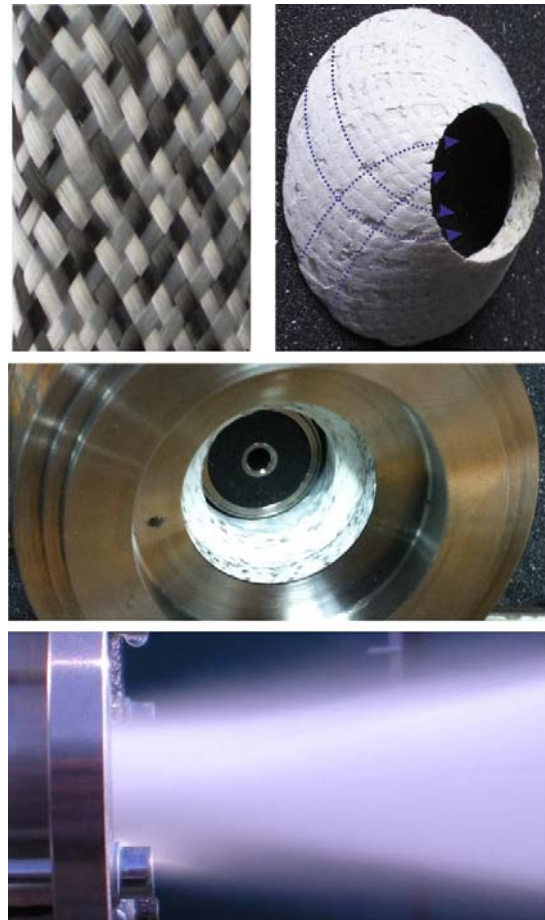


Fig. 19: First generation design of the CMC cone injector. Hybrid woven fabrics as raw material for highly permeable CMC (top left). Oxide injector element for the LOX-injection (top right). Demonstrator (middle). Cold flow test with water (bottom)

This manufacturing procedure, using hybrid woven fabrics, leads to less functional flexibility, because the channel system gets a relatively stochastic array determined by the fibre ply geometry, particularly at the face-plate inflow. An improved manufacturing technology, as given in figure 20, provides high ratio of

functionality in conjunction with the inflow geometry. A basically oxide cone body, made of robust WPS-FW12 material [24] now gets a high definition channel pattern. During manufacturing organic fibres can be inserted well-defined in a highly flexible winding process. The fibres themselves can be defined in their cross section geometry by selection of adequate fibres. The winding angle can be adjusted as well as the number of fibres per ply. A change of winding angle from ply to ply is practicable to get a system of multiple crossing (impinging) LOX jets during firing operation.

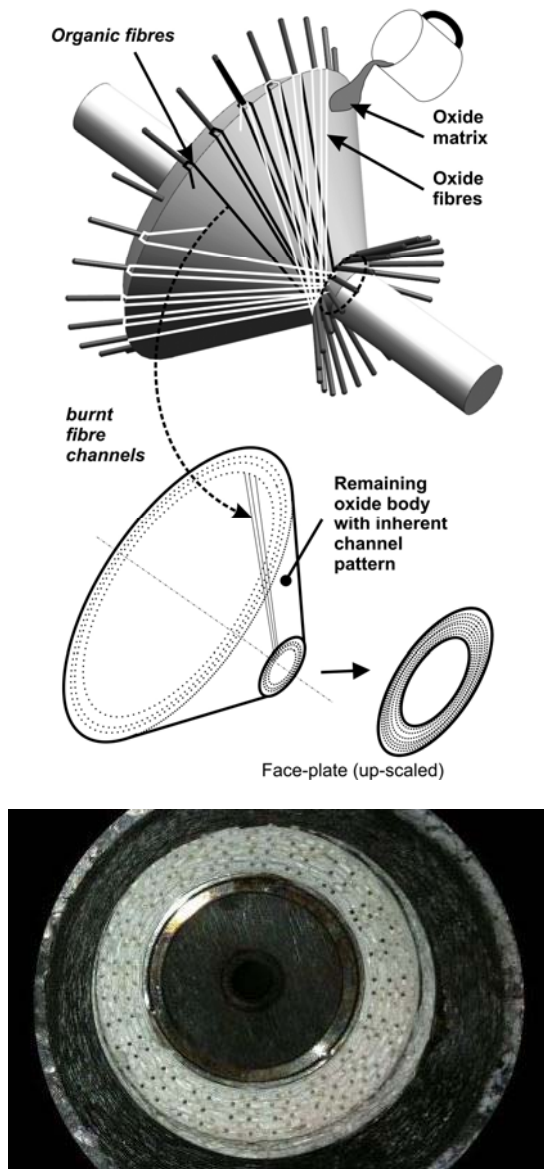


Fig. 20: Improved CMC injector element technology. Winding process (top). Demonstrator element showing high definition injection channel pattern (bottom)

Functional aspects

The high definition channel pattern forms a fine spray of LOX which flows into a cloud of hydrogen, whereas the hydrogen shows ten times higher injection velocity. The goal is an optimized mixing of the oxygen jets themselves. Fine LOX drop patterns flow into the hydrogen cloud and form high ratio of contact surface. As a consequence the mixing process should be performed on a shorter combustion length.

Another interesting aspect is the LOX channel geometry itself. The design intention for the first firing tests at the end of 2013 consisted in the functional adaptation of on the one hand soft ignition and on the other hand stable steady state operation. Hence the channel geometry has been chosen for the following theoretical operational parameters (fig. 21): Long and thin channels (channel diameter 0.4 mm; channel length 15 ÷ 20 mm) should provide a change of phase during the ignition phase for rapid mixing of gaseous oxygen and gaseous hydrogen.

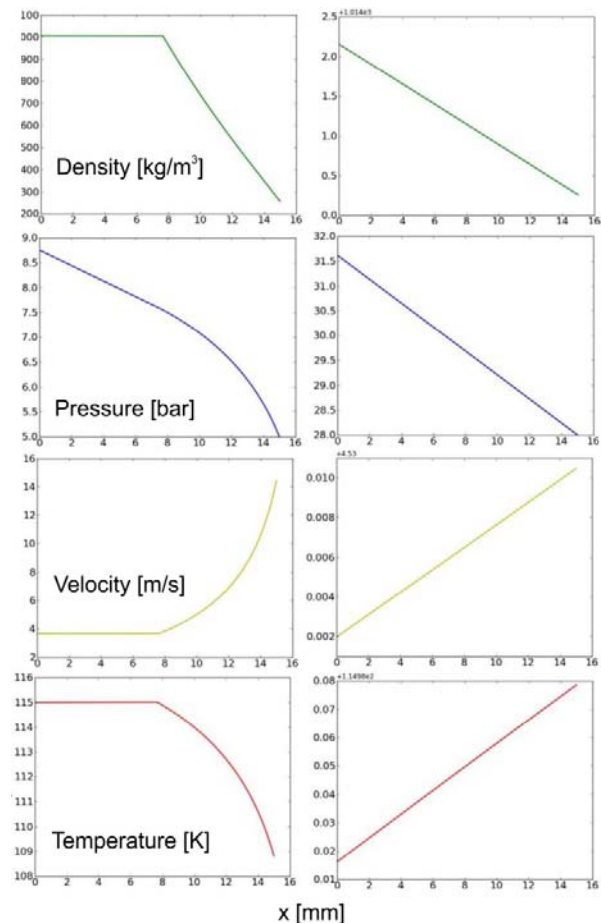


Fig. 21: Two relevant CMC injector channel operations: Start-up with change of phase (left); Steady state, liquid oxygen without change of phase (right)



After ignition the counter pressure from the combustion chamber side compresses the propellants, so that from now on the oxygen remains liquid and higher mass flow at adjusted pressure drops over the face-plate can be fed.

The computed tomography (fig. 22) shows good geometry stability of the single channels after the furnace process for the material consolidation.

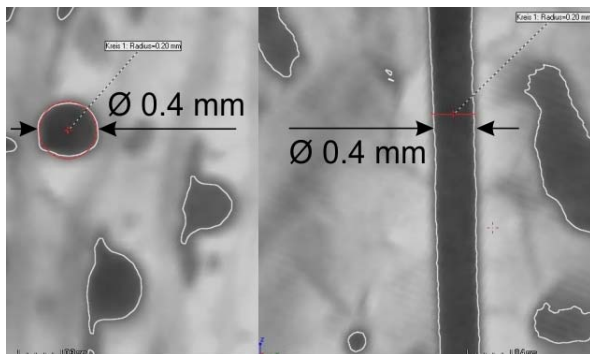


Fig. 22: Good geometry stability of the LOX injection channels in the CMC injector element.

### Experimental results

At the end of 2013 first firing tests of the new CMC injector design could be performed at the P6.1 test facility at DLR Lampoldshausen (fig. 23). Two identical test runs of about 12 seconds duration proved the reproducibility of the function.

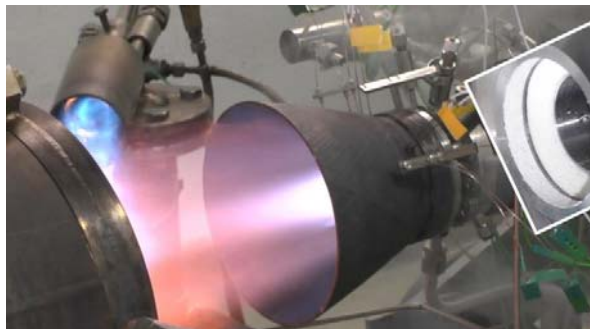
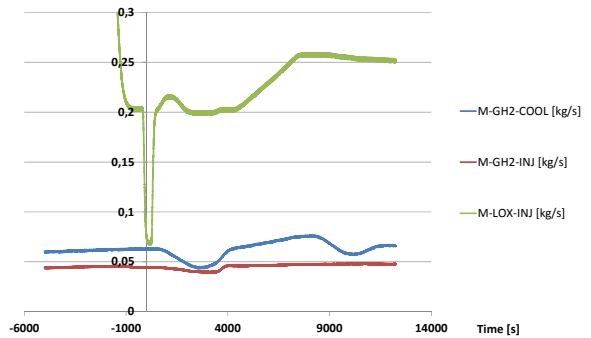


Fig. 23: Cone injector firing test at the P6.1 test facility at 28 bar hot gas pressure.

The chamber pressure amounted to  $p_c = 28$  bar, the propellant mixture ratio at the operational point amounted to  $O/F = 5.3$  and the coolant mass flow ratio of the transpiration cooled CMC chamber amounted to a value of  $\tau = 20$  %. The overall coolant mass flow ratio had been chosen very high for inner chamber wall protection purposes. Coolant mass flow reduction wasn't a test objective in this case. Representative test results of the second test run are given in figure 24. The

LOX mass flow of 255 g/s could be operated at a relatively low pressure drop of  $\Delta p_{LOXinj} = 3$  bar over the CMC element.

DLR - Cone Injector test campaign 'IZ2' - MASS FLOW CURVES



DLR - Cone injector test campaign 'IZ2' - PRESSURE CURVES

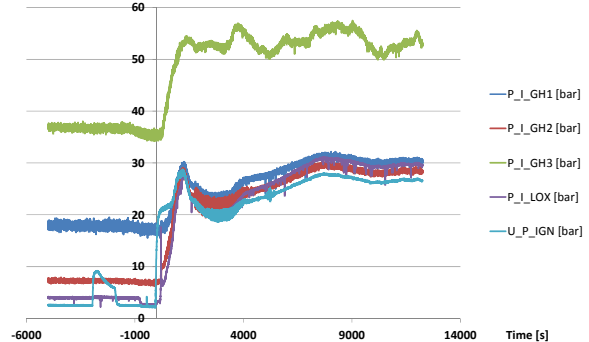


Fig. 24: Cone injector firing test at the P6.1 test facility at 28 bar hot gas pressure. Mass flow (top). Pressures (bottom)

The relatively low pressure loss over the CMC element promises further mass flow increase for higher chamber pressures. The nominal LOX mass flow for this injector design is approximately 600 g/s, targeting on a hot gas pressure of about 60 bar, which should be reached evaluating this test result. In case of pressure drop exceeding the channel pattern could be adapted easily accordingly to higher channel diameters or higher amount of channel numbers without changing the manufacturing process dramatically. The numbers of channels correlates to the number of organic fibres in the raw injector element component, which can be changed easily. The diameter of the channels correlates to the thickness of the organic fibres, which can simply be changed by the suitable selection of fibres.

### V. NOZZLE JOINING METHOD

DLRs ceramic thrust chamber design requires adequate joining techniques between the subsonic chamber body and the supersonic nozzle extension (fig.

23, 25). For this purpose an adapted partial CMC double shell nozzle extension as well as an adjusted hybrid joining method has been developed [4].

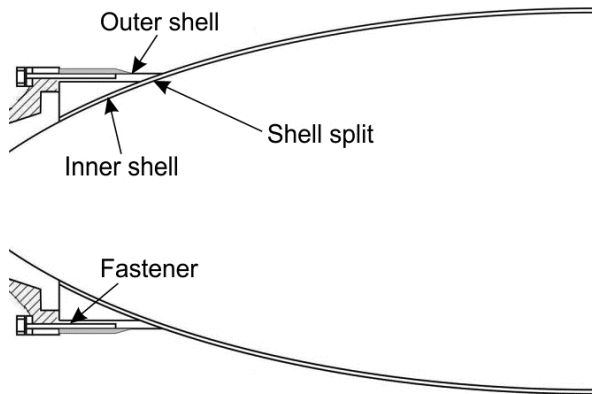


Fig. 25: Principle of the partially double-shelled CMC nozzle extension. Double shell design close to the throat section for thermal and mechanical load decoupling

Close to the nozzle throat section the CMC shell is split into an outer and an inner shell. The outer shell shows a higher mechanical angular impulse and is decoupled from high thermal loads. The inner shell only has to carry the thermal loads and is mechanically weakly loaded.

As joining method a kind of dove tail fastener has been chosen (fig. 26, 27). This metallic fastener shows at the one end the regular screw geometry and at the other end a flat and double step keyed joint.



Fig. 26: Joining elements like dove tails with double-stepped shape at the contact surface for reduction of mechanical stress and strain under thermo-mechanical loading.

The double step keyed joint shows suitable thermo-mechanical compatibility, especially in conjunction with

low mechanical stress levels (fig. 25) and low absolute strains (compared to the one-step-shape) [25].

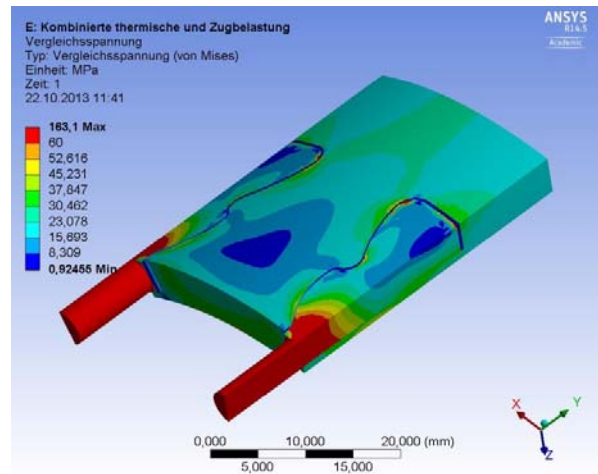


Fig. 27: Cone injector firing test at the P6.1 test facility at 28 bar hot gas pressure. Mass flow (top). Pressures (bottom)

## VI. FUTURE PERSPECTIVES

### Orbital propulsion

Beside transpiration cooled high performance applications the current focus for CMC thrust chamber technology lies on orbital propulsion. For that reason a new hyperboloid subsonic combustion chamber geometry has been investigated (fig. 28). The hyperboloid shape, which idea arose principally from the injection spray shape naturally generated by the CMC cone injector [1, 9], became a highly interesting candidate after first system analysis. Primarily a variety of advantages lies in the CMC specific manufacturing. The hyperboloid structure is convenient for mechanically adjusted fibre winding technology along geodesic lines (typical winding paths (1) and (2), fig. 26).

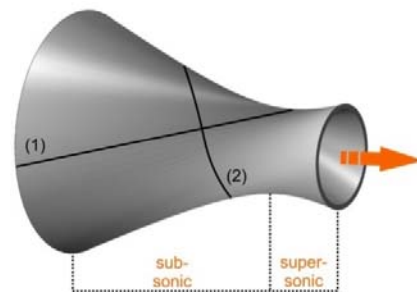


Fig. 28: Hyperboloid combustion chamber geometry with typical fibre winding paths along geodesic lines for an adequate composite manufacturing

Moreover the system analysis gives very interesting indications for the orbital rocket combustion chamber application. A recently finished diploma thesis [23] delivered promising results in conjunction with a comparable film cooled apogee motor. Table 5 displays the specific performance values for the geometry comparison.

|                                    |      |
|------------------------------------|------|
| Chamber length [mm]                | 150  |
| Throat diameter [mm]               | 19   |
| Characteristic chamber length [mm] | 550  |
| Chamber pressure [bar]             | 10   |
| Mass flow [g/s]                    | 163  |
| Thrust [N]                         | 529  |
| Isp [s]                            | 3446 |
| Emissivity [-]                     | 0,9  |

Table 5: Performance parameters of a film cooled apogee thruster for the geometry comparison

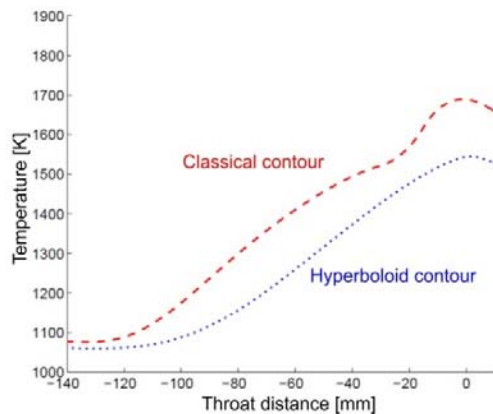


Fig. 29: Thermal performance comparison of the classical and the hyperboloid contour; the latter shows significantly lower inner surface temperatures at the same engine performance

In conjunction with film cooled operation a significant reduction of inner surface temperature peaks of more than 100 K at the critical convergent nozzle section is visible for the hyperboloid contour (fig. 29).

#### Pre-burner technology

Another promising application could be innovative pre-burner technology. Apart from main chamber applications this composite structure system approach is additionally suited for the pre-burner combustion chamber technology for full flow staged combustion (FFSC), whereas the advantage of homogeneous propellant injection through the porous wall component promises system improvements and simplifications respectively (fig. 30).

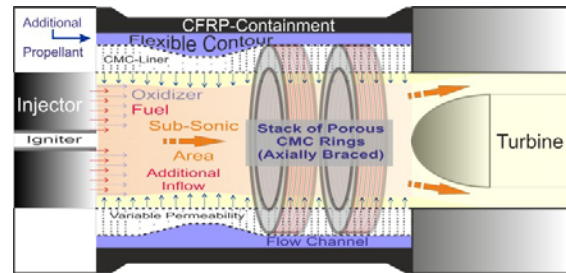


Fig. 30: Design principle of an ox-rich CMC pre-burner

Significantly un-balanced propellant mass flows in the pre-burner can be compensated by convenient use of porous combustion chamber walls. The injector functionality is not affected by critical functional pre-burner-constraints, because the functional inflow requirements can be de-coupled. The inclusion of the porous chamber wall for the propellant injection reduces the injector complexity [17].

#### CMC injector technology

After the demonstration of the principle functionality of the new CMC cone injector improvements can be seen in further adjustments to functional requirements concerning combustion stability, design simplification, throttled systems, hot or cold injection. On the other hand an interesting perspective is the applicability for specific propellant scenarios in for instance hybrid rocket thrusters.

#### Miscellaneous

Future technology improvements can be seen in specific structural hybridization in designing functional thrust chamber components. Combined or complementary designs of CMC and ALM technology seem to be interesting as well as electroplating technology in conjunction with CMCs.

#### VII. CONCLUSION

The general applicability of transpiration cooled cryogenic high performance rocket combustion chambers for LOX/LH<sub>2</sub> operation could now be demonstrated in its fundamentals. Considering scaling aspects high efficiency in a damage free operation has been proved. Relevant test campaigns took place at the European Research and Technology Test Facility P8, as well as at the renewed technology test facility P6.1 (fig. 31). A TRL between 4 and 5 for the combustion chamber component can be stated.

Definition of TRL 4: Component/Subsystem validation in laboratory environment: Standalone prototyping implementation and test. Integration of technology elements. Experiments with full-scale problems or data sets.

Definition of TRL 5: System/subsystem/component validation in relevant environment: Through testing of prototyping in representative environment. Basic technology elements integrated with reasonably realistic supporting elements. Prototyping implementations conform to target environment and interfaces.

Beside the combustion chamber component itself a new CMC injector concept could prove its principle functionality under firing conditions at the P6.1 test facility.

Promising new CMC technologies arise in the field of space propulsion, like innovative orbital propulsion or pre-burner applications.

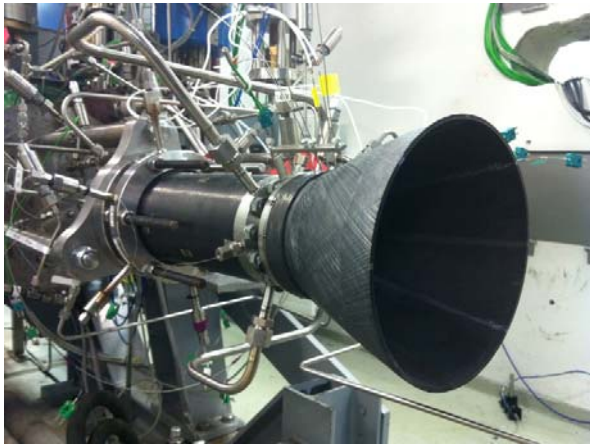


Fig. 31: Continuous subscale CMC rocket thrust chamber within DLR's BlackEngine program at the P6.1 test facility, consisting of CMC injector, CMC/CFRP combustion chamber and CMC nozzle extension

With respect to the complex political and economic structures in Europe today's medium-term perspectives of ceramic space propulsion components will be seen in the orbital or RCS propulsion sector. Also in this field technology improvement becomes visible. Using high temperature capable CMC seems to be promising on the one hand to simplify propulsion structure systems and on the other hand to save cost and rare earth resources. In this specific research field DLR is in close contact with the European space industry like Airbus Defence & Space in the national Propulsion 2020 research network, SNECMA, ONERA and several Universities or other national research institutes.

#### VII. ACKNOWLEDGEMENT

Emphasized thanks for the fruitful institute-internal co-operation shall be given to the department of ceramic composite structures (KVS). Additional thanks have to be given to the institute of space propulsion for the

constructive co-operation in terms of conducting the test campaigns at DLR Lampoldshausen.

#### VII. REFERENCE

- [1] M. Ortelt, A. Herbertz, H. Hald I. Müller. 2013. Advanced Design Concepts for Ceramic Thrust Chamber Components of Rocket Engines. *5<sup>th</sup> EUROPEAN CONFERENCE FOR AERONAUTICS AND SPACE SCIENCES, Munich, Germany.*
- [2] A. Herbertz, M. Ortelt, I. Müller, H. Hald. 2012. Transpiration-Cooled Ceramic Thrust Chamber Applicability for High-Thrust Rocket Engines – Scaling of KSK Test Results. *48<sup>th</sup> AIAA/ASME/SAE/ASEE Joint propulsion Conference & Exhibit, Atlanta, Georgia.*
- [3] M. Ortelt, A. Herbertz, H. Elsässer, H. Hald I. Müller. 2012. Structural Investigations on Cryogenically Operated and Transpiration Cooled Fiber Reinforced Rocket Thrust Chambers. *48<sup>th</sup> AIAA/ASME/SAE/ASEE Joint Propulsion Conference & Exhibit, Atlanta, Georgia.*
- [4] M. Ortelt, F. Breede, A. Herbertz, D. Koch, H. Hald. 2013. Current activities in the field of ceramic based rocket engines. *ODAS 2013- 13<sup>th</sup> ONERA-DLR Aerospace Symposium, Palaiseau, France.*
- [5] A. Herbertz, M. Selzer. 2013. Analysis of Coolant Mass Flow Requirements for Transpiration Cooled Ceramic Thrust Chambers. *29<sup>th</sup> International Symposium on Space Technology and Science, Nagoya, Japan.*
- [6] M. Selzer, S. Schweikert. 2013. Transfer of an analytical transpiration cooling model to the cooling analysis of rocket combustion chambers made of ceramic matrix composites. *5<sup>th</sup> European Conference for Aeronautics and Space Sciences (EUCASS), Munich, Germany.*
- [7] S.R. Ghadiani. 2005. A Multiphase Continuum Mechanical Model for Design Investigations of an Effusion-Cooled Rocket Thrust Chamber. *Research Report 2005-18. Institute of Structures and Design, Stuttgart, Germany.*
- [8] M. Ortelt. H. Hald, A. Herbertz. 2009. Investigations on Fibre Reinforced Combustion Chamber Structures under Effusion Cooled LOX/LH2 Operation. *45<sup>th</sup> AIAA/ASME/SAE/ASEE Joint Propulsion Conference & Exhibit, Denver, Colorado.*
- [9] M. Ortelt. H. Hald, A. Herbertz, W. Rotärmel. 2010. CMC Design Approach for Cryogenic Injector Heads of Rocket Thrust Chambers. *European Conference on Materials and Structures in Aerospace, Berlin, Germany.*

- [10] D. Huzel, D.H. Huang. 1992. *Modern Engineering for Design of Liquid-Propellant Rocket Engines. Volume 147. ISBN 1-56347-013-6.*
- [11] D. Greuel; 2013. Untersuchungen zum Impuls- und Stofftransport in effusiv gekühlten faserkeramischen Raketendbrennkammerwänden. *Dissertation, RWTH Aachen, Germany.*
- [12] J.R. Riccius, D. Greuel, O.J. Haidn, T. Leicht. 2005. Coupled CFD Analysis of the Hot Gas and the Coolant Flow in Effusion Cooled Combustion Chambers. *44<sup>st</sup> AIAA/ASME/SAE/ASEE Joint Propulsion Conference & Exhibit, Tucson, Arizona.*
- [13] J. Lux, D. Suslov, O.J.Haidn. 2008. Experimental Investigation of Porous Injectors for Liquid Propellant Rocket Engines *41<sup>st</sup> AIAA/ASME/SAE/ASEE Joint Propulsion Conference & Exhibit.*
- [14] S. Gordon, B.C. McBride. 2008. Computer Program for Calculation of Complex Chemical Equilibrium Compositions and Applications. Vol. 1: Analysis, NASA, RP-1311.
- [15] M. Lezuo, O.J.Haidn. 2004. Transpiration Cooling H<sub>2</sub>/O<sub>2</sub> – Combustion Devices. *28<sup>th</sup> International Cocoa Beach Conference on Advanced Ceramics and Composites. Cocoa Beach, USA.*
- [16] H. Hald, M. Ortelt, S. Ghadiani, A. Herbertz, D. Greuel, O.J. Haidn. 2003. Application of Fiber Reinforced C/C Ceramic Structures in Liquid Rocket Engines. *International Conference (Space 2003), "Space Challenge in 21<sup>st</sup> Century. 100 Years after the Tsiolkovsky Idea on Space Missions using Reactive Motors", Moscow-Kaluga, Russia.*
- [17] M. Sippel, T. Schwanekamp, M. Ortelt. 2014. Staged Combustion Cycle Rocket Engine Subsystem Definition for Future Advanced Passenger Transport. *Space Propulsion Conference 2014, Cologne, Germany.*
- [18] B. Heidenreich, W. Krenkel, M. Friess, H. Gedon. 2003. Net Shape manufacturing of Fabric Reinforced Oxide/Oxide Components via Resin Transfer Moulding and Pyrolysis. *In: Keramische Verbundwerkstoffe, Weinheim, Wiley-VCH, pp. 48-75.*
- [19] W.E.C. Pritzkow, F. Deuerler, D. Koch, A. Ruedinger, K. Zushtev. 2009. Versagenseffekte auf Grund von Makro-Fehlstellen in Oxidkeramischen Verbundwerkstoffe. *17. Symposium Verbundwerkstoffe und Werkstoffverbunde, Bayreuth, Germany.*
- [20] A. Ruedinger, W. Glaubitt. 2005. Oxidkeramische Matrices basierend auf Sol-Gel-Vorstufen fuer die Herstellung oxidkeramischer Faserverbundwerkstoffe. *cfi/Ber. DKG 82 No. 13, 51-54.*
- [21] M. R. Capra, P. Lorrain, R. R. Boyce, S. Brieschenk, M. Kuhn, H. Hald. 2012. H<sub>2</sub>-O<sub>2</sub> Porous Fuel Injection in a Radical Farming Scramjet. *18<sup>th</sup> AIAA International Space Planes and Hypersonic Systems and Technologies Conference. Tours, France.*
- [22] D. Fricke, 2014. Vergleichende numerische und experimentelle Untersuchung poroeser durchstroemter Medien. *Diplomarbeit, DLR IB 435-2014/29. DLR Institute of Structures and Design, Stuttgart, Germany.*
- [23] T. Schleutker, 2014. Analytischer und numerischer Vergleich des Wärmestroms bei konventionellen und hyperbolischen Brennkammern. *DLR Institute of Structures and Design, Stuttgart, Germany.*
- [24] Kamen, Tushtev. 2012. Charakterisierung von Keramikblech Typ FW12. *Universität Bremen, Fachbereich Keramische Werkstoffe und Bauteile. Bremen, Germany.*
- [25] D. Fricke, 2013. Strukturanalyse einer neuartigen Zapfenverbindung zwischen der faserkeramischen Überschalldüsenerweiterung und der Brennraumkomponente für die faserkeramische Raketenschubkammertechnologie. *Studienarbeit, IRS-13-S73. Universität Stuttgart, Stuttgart, Germany.*